Original Article

PREPARATION AND CHARACTERIZATION OF ALGINATE CHITOSAN CROSSLINKED NANOPARTICLES BEARING DRUG FOR THE EFFECTIVE MANAGEMENT OF ULCERATIVE COLITIS

SHAYMA KHAN[1], NAINA DUBEY[2], BASANT KHARE[3], HARSHITA JAIN[4], PRATEEK KUMAR JAIN[3]

[1]Shri Rawatpura Sarkar College of Prarmacy, Sagar (M. P.), [2]Acropolis Institute of Pharmaceutical Education and Research, Indore (M. P.), [3]Adina College of Pharmacy, Sagar (M. P.), [4]Adina Institute of Pharmaceutical Sciences, Sagar (M. P.)
Email: shyma.inayat@gmail.com

ABSTRACT

Objective: Delivery of anticancer molecule to the liver remains a "holy grail" in molecular medicine and nanobiotechnology with conventional therapy, as conventional cancer chemotherapy does not prove effective as drug molecule does not reach to the target site at therapeutic concentration. Tumor vasculature differs from the vasculature of normal tissue both in morphology and biochemistry. Most of these differences appear too related to angiogenesis (formation of new blood vessels from pre-existing ones). For the present study nanoparticles (NPs) were chosen as a delivery system, because they have many advantages, e. g. they can pass through the smallest capillary vessels because of their ultra-tiny volume, can penetrate cells and tissue gap to arrive at, pH, ion and/or temperature sensitivity of materials, can improve the utility of drugs and reduce toxic side effects.

Methods: PLGA (poly lactide co glycolic acid) was used for the preparation of NPs because of its biodegradability and biocompatibility. It degrades by hydrolysis of ester linkages in the presence of water in to two monomers lactic acid and glycolic acid. There are a number of ligands available for hepatic delivery, among them lactobionic acid (containing galactose moiety) was selected for present work. Preparation of plain nanoparticles was carried out using emulsification–diffusion method. Optimization of the polymer concentration is the first step during the study and it was performed by varying the polymer concentration where as keeping other variables constant. The prepared formulation was optimized on the basis of particle size and polydispersity index. Amount of drug was optimized on the basis of particle size and percentage entrapment efficiency.

Results: Particle size and zeta potential of the nanoparticle were determined by zetasizer showed that particles are in nano range (blow 200 nm) and have acceptable range of zeta potential. Shape and surface morphology were determined by TEM and SEM analysis. The conjugation of lactobionic acid with PLGA polymer was proved by FTIR. The *in vitro* release profiles of entrapped drug from formulations were determined using dialysis membrane. For stability studies, the LDNPs (conjugated NPs) are stored at the temperatures 4±1 °C and room temperature. Human hepatoma cell line HepG2 by SRB assay was selected and it clearly suggests a dose dependent cytotoxicity response i.e. decrease in cell survival fraction with increasing concentration of drug. The *in vivo* study are important in evaluating the targeting efficacy of designed dosage form and also helps in establishing the correlation between the results obtained from *in vitro* experimentation to that from *in vivo* studies. The formulations were administered by tail vein to mice of four groups Group I: PBS 7.4 (control); Group II: 5-FU solution; Group III: DNPs; Group IV: LDNPs.

Conclusion: The proposed targeting strategy is expected to enhance the therapeutic index of conventional anticancer drug as well as reduce its cytotoxic effects to normal cells.

Keywords: Cancer, Nanoparticles, Lactobionic, Cytotoxicity, *In vivo*

INTRODUCTION

Cancer can start within the liver (primary liver cancer or hepatocellular cancer) or spread to the liver (metastatic liver cancer) from other sites, such as the colon. Cancer that starts in the liver is simply called as liver cancer. Liver cancer is the fifth most common cancer in the world. A deadly cancer, liver cancer will kill almost all patients who have it within a year. In 2008, the World Health Organization estimated that there were about 830,000 new cases of liver cancer worldwide, and a similar number of patients died as a result of this disease [1-5]. About three quarters of the cases of liver cancer are found in Southeast Asia (China, Hong Kong, Taiwan, Korea, and Japan). Liver cancer is also very common in sub-Saharan Africa (Mozambique and South Africa). The frequency of liver cancer in South-East Asia and sub-Saharan Africa is greater than 30 cases per 100,000 populations. In contrast, the frequency of liver cancer in North America and Western Europe is much lower, less than 8 cases per 100,000 populations. However, the frequency of liver cancer among native Alaskans is comparable to that seen in Southeast Asia. Moreover, recent data show that the frequency of liver cancer in the U. S. overall is rising [6-8].

Nanoparticles are subnanosized colloidal carrier system composed of synthetic, semisynthetic or natural polymers in the size range of about 10-1000 nm [9].

Two types of nanoparticulate systems are possible;

• Matrix type-drug is dispersed homogenously into the entanglement of oligomers or polymeric units.

Ex. Nanospheres

• Reservoir type–oily core of drug is surrounded by the embryonic polymeric shell.

Ex. Nanocapsules

Hepatocellular carcinoma (HCC) is third cause of cancer related death. In Asia and Africa, high incidence rates of HCC have been associated with high endemic hepatitis B carrier and with mycotoxin contamination of food stuffs, stored grains, drinking water and soil [10-13].

Several strategies including surgery, percutaneous/intravenous/ ablations, radiation and chemotherapy and other newer therapy including gene therapy, either alone or in combination are used for the treatment of HCC. In early age, surgical resection and liver transplantation had been used but it was possible only in 30% cases with those diagnosed with small tumour burden. Moreover, chances of recurrence are very high. Therefore, over the years, research in drug delivery systems has been focused on development of novel and target specific drug delivery systems for effective localization of

active drug moiety in to vicinity of preidentified target in therapeutic concentration while restricting its access to non target normal tissues. This strategy minimizes the toxic effects and maximizes the therapeutic index [14-17].

In present paper, lactobiotin anchored PLGA nanoparticles bearing anticancer drug shall be designed and developed for liver tumour specific delivery of anticancer drug. The lactobiotin molecule shall be recognized by the liver associated surface receptors i.e. asialoglycoprotien receptor (galactose receptor) which are appended at the surface of nanoparticle. The galactose moiety of the lactobionic acid targets to the tumour cells in the liver. Nanoparticles offer additional advantages as drug carrier for cancer targeting due to their nano-metric size range and high drug loading propensity. The proposed targeting strategy is expected to enhance the therapeutic index of conventional anticancer drug as well as reduce its cytotoxic effects to normal cells [18, 19].

PLGA (poly lactide co glycolic acid) was used for the preparation of NPs because of its biodegradability and biocompatibility. It degrades by hydrolysis of ester linkages in the presence of water in to two monomers lactic acid and glycolic acid which under normal physiological condition, are by-products of various metabolic pathways in the body. PLGA with 50: 50 monomers and molecular weight 17000 was used in this work. It has very good mechanical properties and long shelf-life. For this study uncapped PLGA was used, having free carboxylic acid group (COOH) for the conjugation [20-24].

Preparation, optimization and characterization of nanoparticles

MATERIALS AND METHODS

PLGA Poly (d,l–lactide–co–glycolide) and 5-FU were obtained as a gift sample from Sun Pharma (Vadodra) and Biochem Pharmaceuticals industries ltd., Daman, respectively. Pluronic F-68 (PF-68), Triton X-100, dialysis membrane (MWCO 6,000–7,000 Da) were purchased from Himedia, Mumbai, India. Lactobionic acid is purchased from Sigma-Aldrich Chemicals Pvt. Limited, Banglore. All other reagents and solvents used were of analytical grade unless stated otherwise double distilled water was used throughout the study.

Preparation of nanoparticles

• Preparation and optimization of plain and drug loaded PLGA nanoparticle

• Preparation and optimization of drug loaded lactobionic acid-PLGA nanoparticle

Preparation of PLGA nanoparticle

The nanoparticle was prepared using the emulsification-diffusion method [25].

Procedure

According to this method, the organic phase (PLGA in ethyl acetate) was added into an aqueous phase (Pluronic F-68 in distilled water or PBS 7.4 or drug). After mutual saturation, the mixture was emulsified with a probe sonicator. In order to allow diffusion of the organic solvent in to water, a constant volume of water was subsequently added to the o/w emulsion under magnetic stirring, leading to the formation of PLGA nanoparticles [26, 27].

Optimization

There are various formulation and process variable, which could affect the preparation and properties of nanoparticles. These formulation variables were identified and optimized to get uniform preparation with highest encapsulation efficiency. Formulation variables include amount of drug, polymer concentration and stabilizer concentration and process variables include stirring speed, stirring time and sonication time. All these parameter were optimized by taking the effect of variable on particle size, polydispersity index and encapsulation efficiency [28-30].

Effect of polymer concentration

Polymer (PLGA) concentration was optimized using their different concentration of PLGA (0.5%, 1.0%, 1.5%) while other parameters remained constant and the optimum value was identified on the basis of average particle size and polydispersity index (PDI) of nanoparticles, which were determined using Malvern Zetasizer [31]. Results are shown in table 1.

Effect of stabilizer concentration

For the optimization of stabilizer concentration, nanoparticle formulation NP-2 was selected and different nanoparticle formulations were prepared with varying concentration of stabilizer pluronic F-68 (viz. 0.5%. 1.0%, 1.5%, 2.0%) keeping the other parameters constant. Optimization was done on the basis of average particle size of nanoparticles [32, 33]. Results are shown in table 2.
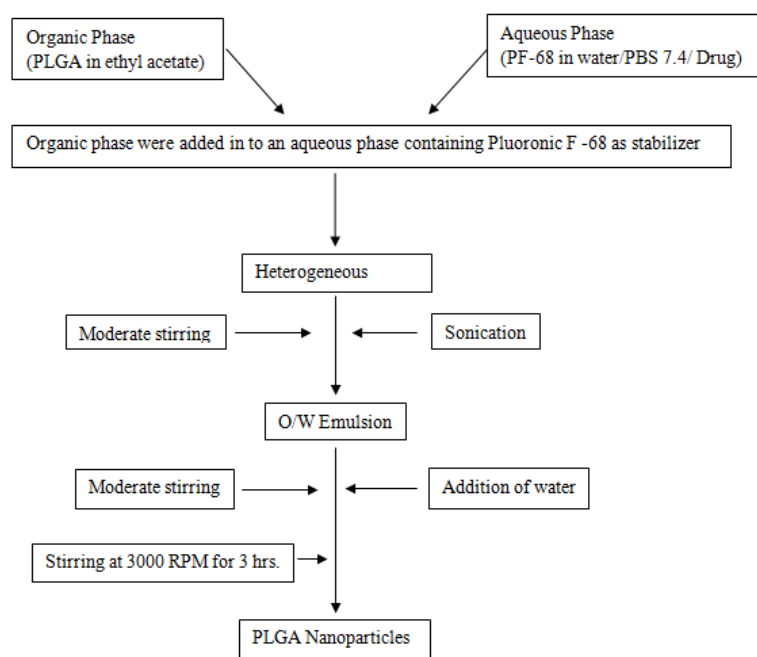
Scheme 1: Preparation of PLGA nanoparticles

Table 1: Effect of polymer concentration

S. No.	Formulation code	Polymer concentration	Particle size (nm)	PDI
1.	NP-1	0.5%	101.34±2.3	0.518
2.	NP-2	1.0%	106.24±2.1	0.361
3.	NP-3	1.5%	142.38±2.2	0.486

Values represent mean±SD n= 3

Table 2: Effect of stabilizer concentration

S. No.	Formulation code	Stabilizer concentration	Particle size (nm)	PDI
1.	NP2S-1	0.5%	120.98±1.6	0.378
2.	NP2S-2	1.0%	112.36±2.1	0.321
3.	NP2S-3	1.5%	121.89±1.5	0.474
4.	NP2S-4	2.0%	125.67±2.4	0.585

Values represent mean±SD n= 3

Optimization of concentration of drug

Encapsulation efficiency is the major parameter for nanoparticle formulation so it was optimized by varying the drug concentration (5, 10 and 15 mg) in the above selected formulation NP2S2 and keeping the other parameters constant. Optimization was done on the basis of average particle size of nanoparticle and percent drug entrapment [34]. Results are shown in table 3.

Optimization of stirring speed

The size of nanoparticles depend on the stirring speed and it is optimized by preparing different formulation with varying stirring speed (2000, 3000 and 4000 rpm.) [35] Results are shown in table 4.

Optimization of stirring time

Stirring time optimization for selected formulation (NP2S2D2S-2) was performed by varying stirring time, during formulations. Further the particle size and percent drug entrapment were determined [36]. Results shown in table 5.

Optimization of sonication time

Particle size reduction to nanometric size and their uniformity is very important parameter for nanocarrier and it can be achieved by sonication process, their size reduction depend on the time of sonication. It is optimized by varying sonication time (30, 60, 90 sec.) during formulation. Further the particle size and percent drug entrapment were determined [37].

Table 3: Optimization of concentration of drug

S. No.	Formulation code	Concentration of drug (mg)	Particle size (nm)	% Entrapment efficiency
1.	NP2S2D-1	5	108.63±2.5	50.46±1.7
2.	NP2S2D-2	10	110.45±5.4	64.67±2.2
3.	NP2S2D-3	15	115.23±2.3	64.63±2.5

Values represent mean±SD n= 3

Table 4: Optimization of stirring speed

S. No.	Formulation code	Stirring speed (rpm)	Particle size (nm)	%Entrapment efficiency
1.	NP2S2D2S-1	2000	125.42±2.1	62.89±2.3
2.	NP2S2D2S-2	3000	111.71±3.4	63.67±2.4
3.	NP2S2D2S-3	4000	117.15±2.3	64.98±1.9

Values represent mean±SD n= 3

Table 5: Optimization of stirring time

S. No.	Formulation code	Stirring time (h)	Particle Size (nm)	%Entrapment Efficiency
1.	NP2S2D2St-1	2	128.78±2.1	61.89±2.5
2.	NP2S2D2St-2	3	114.34±2.3	64.67±1.6
3.	NP2S2D2St-3	4	116.67±2.5	67.78±2.1

Values represent mean±SD n= 3

Table 6: Optimization of sonication time

S. No.	Formulation code	Sonication time (sec.)	Particle size (nm)	%Entrapment efficiency
1.	NP2S2D2S2S-1	30	134.56±2.3	64.23±2.4
2.	NP2S2D2S2S-2	60	115.73±2.1	62.38±2.3
3.	NP2S2D2S2S-3	90	125.37±2.6	53.36±2.1

Values represent mean±SD n= 3

Preparation and characterization of lactobionic acid conjugated PLGA nanoparticle

Preparation

The conjugation of lactobionic acid to the PLGA was done in three steps

• Introduction of amine terminal to the PLGA via conjugation of ethylene diamine

• Activation of carboxylic group of lactobionic acid

• Carboxylic group of lactobionic acid was conjugated to free amine group of amine terminated PLGA

Introduction of amine terminal to the PLGA via conjugation of ethylene diamine

PLGA (100 mg) was dispersed in 5 ml of distilled water and placed it in an ice bath. Further ethylene diamine EDA (80 µl) was added then aqueous solution of 1-ethyl-3 dimethylamino propyl carbodiimide hydrochloride (EDC) 250 mg/2 ml was added and adjusted to pH 5

using 1N HCL. The solution slowly stirred for overnight than dialysed against distilled water for 24 h using dialysis membrane (6-7KD).

Activation of carboxylic group of lactobionic acid

Lactobionic acid, N,N'-dicyclohexyl carbodiimide (DCC), N-hydroxysuccinimide (NHS) separately dissolved in dimethyl sulfoxide (DMSO). DCC/DMSO solution added to lactobionic acid solution and stirred for 30 min to activate carboxylic group of the lactobionic acid, then NHS/DMSO solution added to activated lactobionic acid solution and reaction is conducted at room temperature for 12 hour. In reaction mixture, dicyclohexylurea (DCU) was formed, which was filtered to remove DCU. By this procedure carboxylic group of lactobionic acid is activated.

COOH group of lactobionic acid was conjugated to free amine group of amine terminated PLGA

Activated lactobionic acid solution was slowly added to amine terminated PLGA solution and slowly stirred for two days. The resulting solution was extensively dialyzed using dialysis membrane (MWCO 6KD) [38-40].
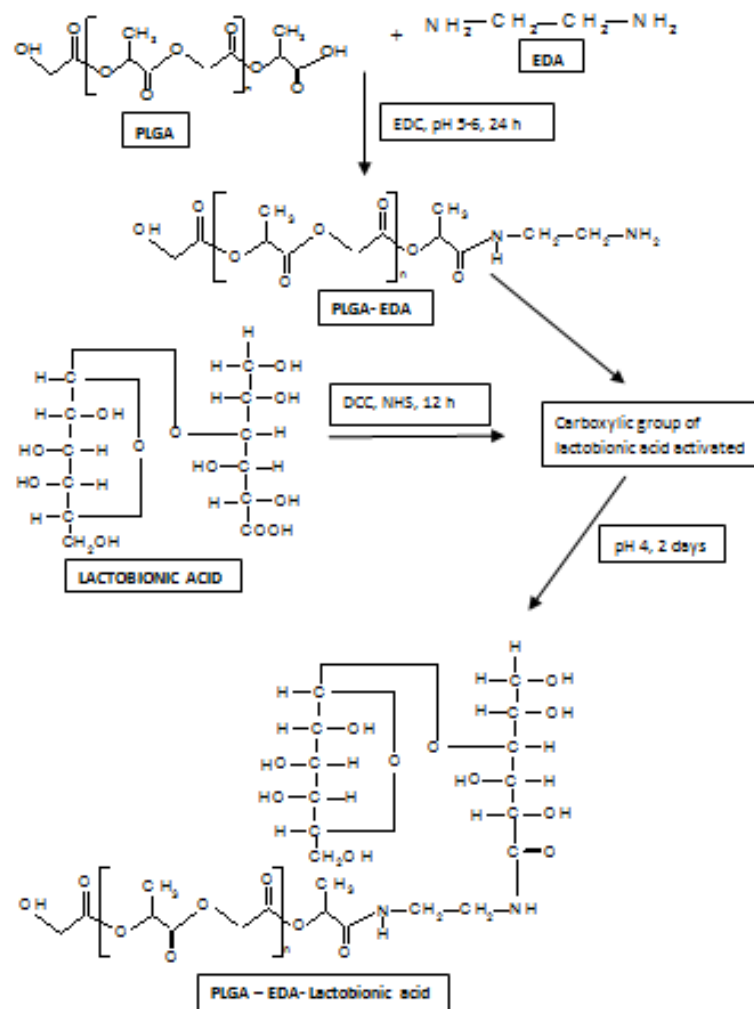

Fig. 1: Strategy for ligand conjugation

Characterization of PLGA-lactobionic conjugates

By FT-IR

Fourier transform infrared specterophotometry (FTIR spectrometer, BRURER IFS-55, Switzerland) was used to study the conjugation

between PLGA and ethylene diamine and galactose moiety of lactobionic acid. The IR spectra of PLGA, PLGA-EDA and PLGA-EDA-Lactobionic were taken using the KBr method, which are shown in fig. 4.8 to 4.10. The characteristic bands in IR spectrum are recorded in table 4.7 to 4.9.
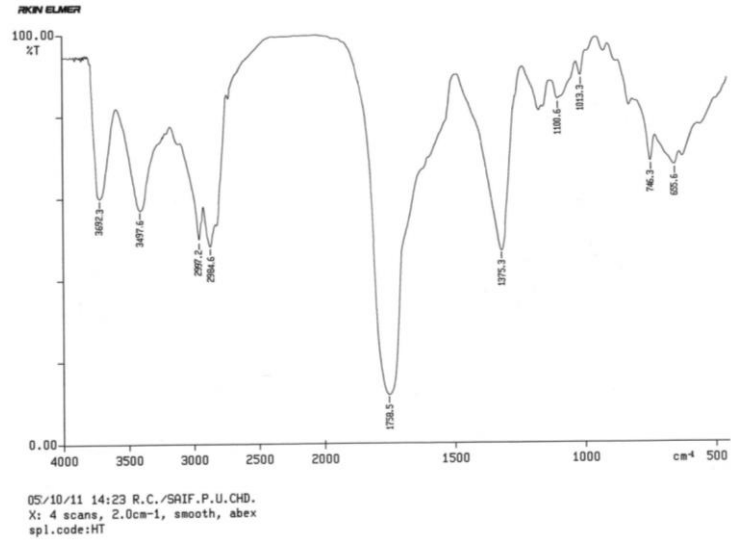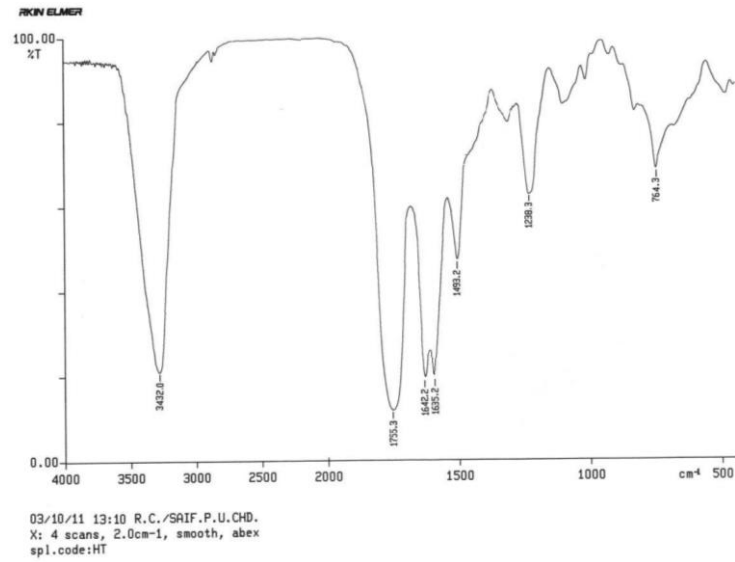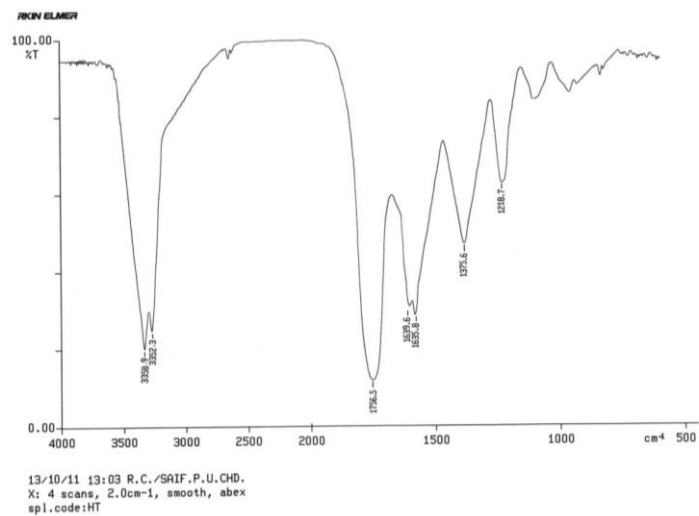
Fig. 2: FT-IR of PLGA

Fig. 3: FT-IR of PLGA-EDA

Fig. 4: FT-IR of PLGA-EDA-lactobionic

Table 7: Optimized parameters for PLGA nanoparticles

S. No.	Parameter	Optimized value
1.	Polymer concentration	1%
2.	Stabilizer concentration	1%
3.	Amount of drug	10 mg
4.	Stirring speed	3000rpm
5.	Stirring time	3 h
6.	Sonication time	60 sec

Table 8: Characterization of optimized formulation

S. No.	Formulation code	System	Zeta potential (mv)	% Entrapment efficiency	Particle size (nm)	PDI
1.	NPs	NPs	-15.34	ND	110±1.3	0.321
2.	DNPs	FU-NPs	-14.29	63.46±1.7	115±2.5	0.345
3.	LDNPs	L-FU-NPs	-13.87	60.23±1.3	117±1.8	0.368

ND= Not detected

Optimized parameters

The various optimization studies were performed during nanoparticle preparation and formulation code is designed as NP2S2D2S2S-2 and the different parameter used for the preparation of optimized formulation are shown in table.

Optimized preparation

For convenience, the formulation code of optimized formulation NP2S2D2S2S-2 was recorded as LDNPs

Characterization of nanoparticles

Particle size and surface charge measurement

Average particle size and surface charge potential of NPs were determined using a Zetasizer (DTS ver. 4.10, Malvern Instruments, England). The particle size distribution is represented by the average size diameter. The surface charge of nanoparticle was determined by measurement of zeta potential (Ɛ) of the nanoparticle and calculated according to Helmholtz–Smoluchwsky from their electrophoretic mobility.

Particle morphology

Transmission electron microscopy (TEM)

Transmission electron microscopy was performed using a Philips CM 10 electron microscope, with an accelerating voltage of 100 kv. A drop of the sample was placed on a carbon coated copper grid to leave a thin film on the grid. Before the film dried on the grid, the film was negatively stained with 1% phosphotungstic acid (PTA). A drop of the staining solutions was added on to the film and the excess of the solution was drained off with a filter paper. The grid was allowed to air dry thoroughly and samples were viewed under a transmission electron microscope and photographs were taken at suitable magnification (Photomicrograph 1)

**Surface morphology (SEM)**

Surface morphology was determined by Scanning Electron Microscope (SEM) at AIIMS, New Delhi. The samples for SEM were prepared by lightly sprinkling the SLN powder on a double adhesive tape, which was stuck on an aluminium stub. The stubs were then coated with gold to a thickness of about 300 °A by using a sputter coater. All samples were examined under a scanning electron microscope (LEO 435 VP, Eindhoven Netherlands) at an acceleration voltage of 30 kV, and photomicrographs were taken at suitable magnification, which are shown in (Photomicrograph 2)

Encapsulation efficiency

Entrapment efficiency of the drug 5-fluorouracil in NPs was determined by using Sephadex G–50 mini column. To prepare Sephadex G–50 mini column, firstly 500 mg of Sephadex G–50 was allowed to swell in 0.9 % NaCl aqueous solution for 8 h and then the hydrated gel was filled in the barrel of 2 ml disposable syringe plugged with filter pad and glass wool. The barrel was centrifuged at 2000rpm for 2 min to remove excess of saline solution from the Sephadex column.
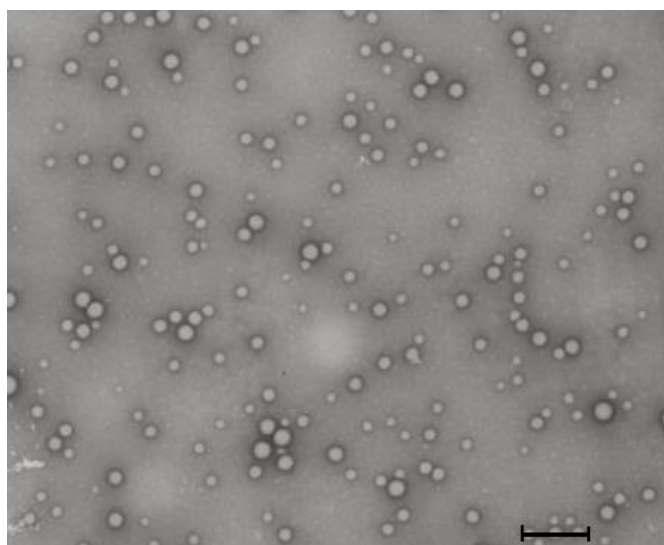
Photomicrograph 1: TEM of PLGA nanoparticle
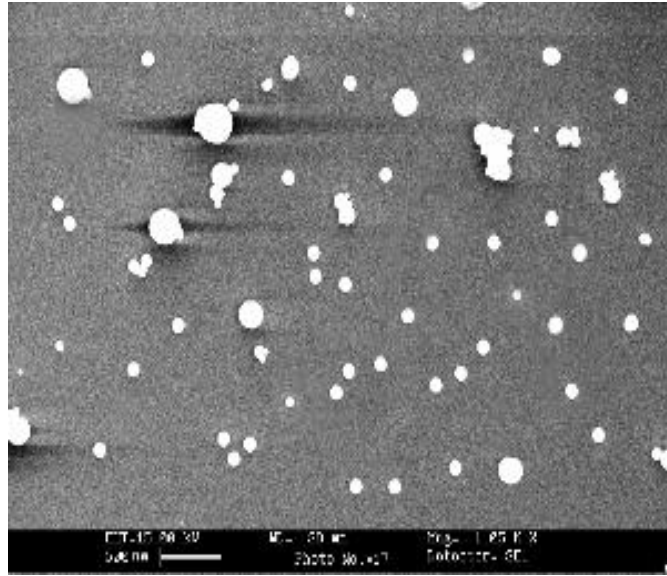
Photomicrograph 2: SEM of PLGA nanoparticle

To separate free drug from NPs formulation 2 ml of NPs dispersion was applied drop wise on the top of the Sephadex column and then centrifuged at 2000 rpm for 2 min., to expel and remove void volume containing NPs. This eluted NPs dispersion was collected and lyses by disrupting with 0.1% Triton X-100 and then the amount of entrapped drugs was analyzed using spectrophotometric method. The amount of drugs entrapped in conjugated NPs was determined employing similar procedure as reported for drugs loaded nanoparticles.

$$\% \text{ Entrapment efficiency} = \frac{\text{Weight of total drug} - \text{Weight of free drug}}{\text{Weight of total drug}} \times 100$$

Cumulative percent drug release

The *in vitro* drug release of entrapped drug from NPs formulation was determined using dialysis tube method. The NPs formulation was first separated from free drug by passing through Sephadex column and then subjected to centrifugation. Separated NPs formulation (5 ml) was taken in to the dialysis tube (molecular weight cut off 13 KDa, Himedia, India) and placed in a beaker containing 100 ml of PBS (pH 7.4). The beaker was placed over a magnetic stirrer and the temperature was maintained at 37±1 ℃ throughout the procedure. Samples were withdrawn at definite time intervals and replaced with same volume of fresh phosphate buffer solution pH 7.4. It was then analyzed for drug content spectrophotometrically.

The rate of drug release in PBS (pH7.4) was observed as controlled release pattern, due to ability of degradative nature of polymer. The release rate from LDNPs was found to decrease because of steric hindrance.
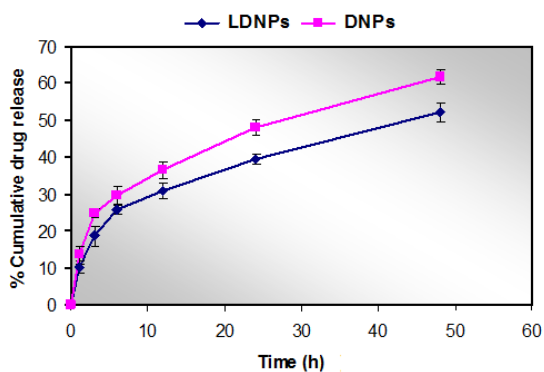

Fig. 5: Cumulative percent drug release

Stability

The significance of stability testing in the development of pharmaceutical dosage forms is well recognized in the pharmaceutical field. The purpose of stability testing is to provide evidence on how the quality of a drug substance or drug product varies with time, under the influence of a variety of environment factors such as temperature, humidity and light and to establish a re-test period for the drug substance or a shelf life for the drug product and recommended storage condition.

The stability of a dosage form is usually defined as the capacity of the formulation to remain within defined limits over a predetermined period of time and is known as shelf life of the product. Stability of a formulation may also be defined as the capability of a particular formulation packaged in a specific container to remain within its physical, chemical, microbiological, therapeutic and toxicological specifications. A stable drug delivery system should maintain its integrity and morphology, and at the same time should preserve various characteristics such as nature of the entrapped drug, drug content and release rate etc. In most of the stability studies, the major emphasis has been directed towards the accelerated stability studies but the stability studies of aged products have been of greater pharmaceutical significance

The stability of the drug-loaded nanoparticles during storage is undoubtedly another important prerequisite for its successful clinical application. Degradation is likely to occur under topical prepared nanoparticles were subjected to accelerated stability testing (41).

Effect of storage on particle size

Size of the NPs was determined at 10 d interval up to 60 d at 4±1 °c and room temperature (about 25 °C) by quasielastic laser light scattering using a Zetasizer DTS Ver. 4.10 (Malvern Instruments, UK). Effect of storage on the size of the particle has been shown in (table 5.1, 5.2 and fig. 5.1, 5.2).

Effect of storage on residual drug content

Entrapment efficiency of stored NPs dispersion was determined after 10, 20, 30, 45 and 60 d, and percent residual drug content was calculated. The entrapment efficiency was determined after separation of the unentrapped drug by the use of the dialysis membrane tubing (MWCO 6-8 kDa, Sigma, USA), thus only the free form of the drug was released through the membrane into the dissolution medium, and the drug within the NPs was retained within the dialysis membrane tubing. The amount of free drug was determined using spectrophotometric technique (table 5.3, 5.4 and fig. 5.3, 5.4).

Table 9: Effect of storage on the particle size of LDNPs at 4±1 °C

Formulation code	Particle size (nm) after storage for					
	Initial	10 d	20 d	30 d	45 d	60 d
NP2S2D2S2S-2	117±1.8	118±1.3	121±1.2	124±1.5	126±1.4	128±1.4

SD±mean (n=3)

Table 10: Effect of storage on the particle size of LDNPs at room temperature

Formulation code	Particle size (nm) after storage for					
	Initial	10 d	20 d	30 d	45 d	60 d
NP2S2D2S2S-2	117±1.8	121±1.2	130±1.5	133±1.3	138±1.8	141±1.2

SD±mean (n=3)

Table 11: Effect of storage on the residual drug content of LDNPs at 4±1 °C

Formulation code	Residual drug content after				
	10 d	20 d	30 d	45 d	60 d
NP2S2D2S2S-2	99.12±1.4	98.29±1.2	97.50±0.7	96.47±1.6	95.33±1.3

SD±mean (n=3)

Table 12: Effect of storage on the residual drug content of LDNPs at room temperature

Formulation code	Residual drug content after				
	10 d	20 d	30 d	45 d	60 d
NP2S2D2S2S-2	97.22±1.2	96.46±0.2	94.29±1.1	91.17±1.4	88.92±0.4

SD±mean (n=3)

In vivo studies

The *in vivo* studies are important in evaluating the efficacy of designing dosage form. The *in vivo* performance is the preliminary step for clinical evaluation of a drug. There are many ways to assess the *in vivo* performance i.e. measuring the intact drug or metabolite level in the blood or urine assessing the physiological and biological response in laboratories animals or by measuring tissues or organs distribution of drug. It is difficult to predict the behavior of a dosage form on the basis of *in vitro* studies. Hence *in–vivo* studies in animal or human volunteers are most important before the product is introduced into the market. On the basis of optimization and *in vitro* characterization of the formulations DNPs (unconjugated NPs) and LDNPs (conjugated NPs) were selected for *in vivo* evaluation.

Selection of animals

Balb/c mice of either sex were used for the present *in vivo* studies. The mice were maintained on standard diet and water. Healthy mice of uniform body weight (18-22 g) with no prior drug treatment were used for these studies. The protocol was duly approved by the Institutional Animal Ethical Committee of Dr. H. S. Gour Central University, Sagar, M. P. (Protocol No: Animal Eths. Comm./11/10).

The prepared drug delivery system was administered intravenously (i. v.) in equivalent amount of Drug (5-FU) to mice and performed the comparison between drug plasma concentration profile and tissue distribution time profile with data obtained from administration of plain drug solution to albino mice.

Study design

Balb/c mice were divided into four groups, in which the first group having one mice served as a control, the other three groups having three mice in each group. In which the second group received free drug solution, third and fourth groups received unconjugated and conjugated formulations, respectively. They were fasted overnight before administration of dose. The dose of the drug administered by intravenous route through tail vein in mice was 12 mg/kg body weight. Unconjugated and lactobionic acid conjugated nanoparticles were administered to each mice of third and fourth group, respectively. After administration of formulation, one rat from each group was sacrificed after 2 h, 8 h and 24 hour. Blood samples were collected through cardiac puncture. Different organs i.e. kidney, liver, spleen and brain were isolated and dried with tissue paper and weighed. The organs were excised and homogenized in 0.4% ortho phosphoric acid in methanol, PBS pH 7.4 mixture. The organic extracts were separated by centrifugation at 1200rpm for 10 min, filtered and dissolved in mobile phase (Potassium dihydrogen phosphate). One ml of this solution was filtered through 0.45 μm membrane filter. The amount of drug presents in each organs and blood samples were determined using HPLC method.

Estimation of drug in serum

Blood sample was collected through cardiac puncture in a centrifuge tube which contains heparin (anticoagulant) and centrifuged at 5000 rpm for 10 min. Supernatant was collected, then added 2 ml of 0.4% ortho–phosphoric acid and was deprotenized with equal amount of acetonitrile for half an hour to precipitate proteins. The precipitated proteins were separated by centrifugation at 5000rpm for 10 min and supernatant was collected and filtered through 0.45 μm membrane filter. Same procedure was followed for unconjugated and conjugated NPs administered mice. The filtrate (25 μl) was injected into a C_{18} (mu) HPLC column and the eluents were monitored at 260 nm with a flow rate 1 ml/min. The peak area of drugs was recorded, the regression of plasma serum concentration of the drug over its peak areas were calculated using the least square method of analysis.

Estimation of drug in various organs

The HPLC method was used for quantification of drug in different organs of balb/c mice. Balb/c mice were sacrificed after specified time intervals and organs were isolated, dried using tissue paper (liver, spleen, kidney and lung). The organs were excised, weighed and minced into small pieces. One gram of each organ was homogenized with 2.0 ml of 0.4% ortho phosphoric acid in methanol, PBS pH 7.4 mixture. If the organs weighing less than one gram then whole organ was used. In the tissue homogenate 2.0 ml of acetonitrile was added and kept aside for 30 min then resultant suspension was centrifuged for 30 min at 3000 rpm and filtered through 0.45μm membrane filter. Supernatant of tissue homogenates were analyzed for drug content similarly as described in drug estimation in serum.
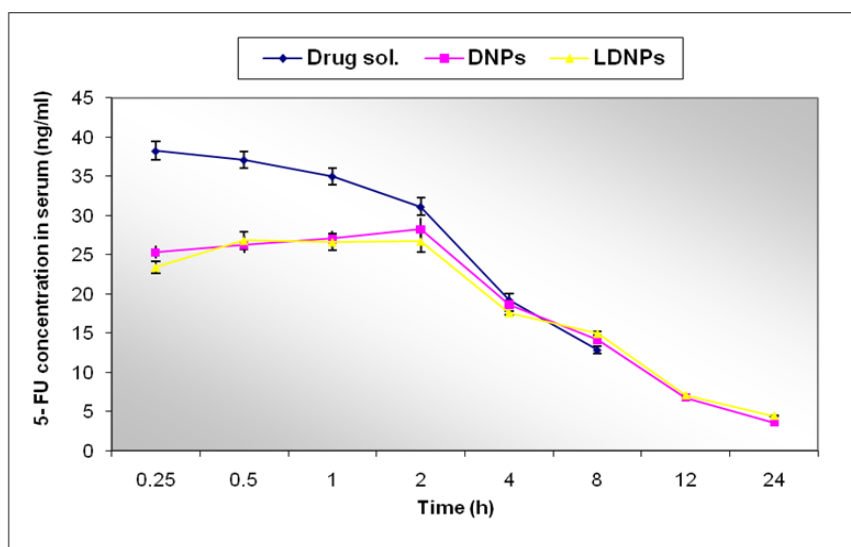
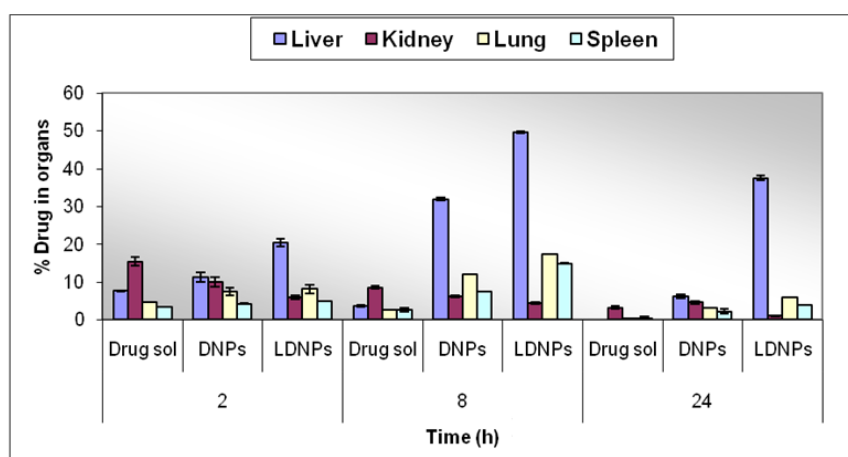Fig. 6: Drug serum profile in various time intervals

Fig. 7: Biodistribution of formulations in various organs of mice

Fluorescence microscopy

Imaging modalities that are non-invasive and *in vivo* have become especially important to study animal models longitudinally. Broadly, these imaging systems can be categorized into primarily morphological/anatomical and primarily molecular imaging techniques. Techniques such as high-frequency micro-ultrasound, magnetic resonance imaging (MRI) and computed tomography (CT) are usually used for anatomical imaging, while optical imaging (fluorescence and bioluminescence), positron emission tomography (PET), and single photon emission computed tomography (SPECT) are usually used for molecular visualizations [42, 43].

The fluorescence microscopy was performed in order to confirm the drug uptake by the different organs from the plain solution, unconjugated and conjugated nanoparticles to help in qualitative assessment of formulation to reach the liver comparative to other organs. FITC (Fluorescein isothiocyanate) was used as fluorophore, which was encapsulated into the unconjugated DNPs and conjugated LDNPs nanoparticles in place of drug and the formulations were administered to balb/c mice intravenously through tail vein. Mice were sacrificed after 4hr and different parts i.e. Liver, kidney, lung and spleen, were excised from these animals and isolated. They were cut into small pieces and washed in Ringer's solution with subsequent drying using tissue paper. Dried pieces of various organs were fixed in Carnay's fluid (absolute alcohol: chloroform: glacial acetic acid, 3.5: 1: 0.5).

Dehydration of liver and other tissues

The dried organ pieces were transferred from Carnay's fluid to the absolute alcohol for dehydration. Procedure was repeated thrice after each 30 min interval.

Paraffin infiltration and embedding

After dehydration, the tissues were transferred to a mixture of alcohol: xylene (1:1) for 1 hour, after which they were kept in xylene for 2 hr. Then wax scrapings were added to xylene up to the saturation level and kept undisturbed for 12 h. The molten matured wax, free of any suspended particles was kept in first infiltration pan kept in the incubator at 62-64 °C for one day. The tissue was then transferred to molten matured wax in first infiltration pan kept in incubator at 62-64 °C. The tissue was then transferred to the second and third infiltration pans each after 30 min maintained at 62-64°C.

### Preparation of block and microtomy

The blocks were prepared using the lid of Cuffling's jar. Filtered melted wax was poured in the lid up to 4/5th of its total height. The tissues were removed from the infiltration pans and placed gently into the lid. They were allowed to stand at room temperature till solidified. The lid was placed in the tray containing water. They were kept as such, till the blocks separated and blocks floated in water. The blocks were cut and trimmed to remove the excess wax. Then microtomy was done with the help of microtome and ribbons of the

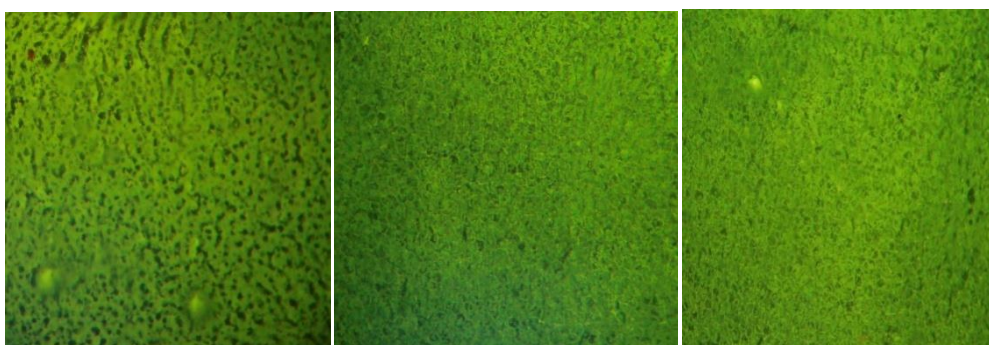sections obtained were fixed on the slides using egg albumin solutions as fixative [44]. The sections were viewed under fluorescence microscope and photomicrographs were taken and shown as (photomicrographs 7.1)
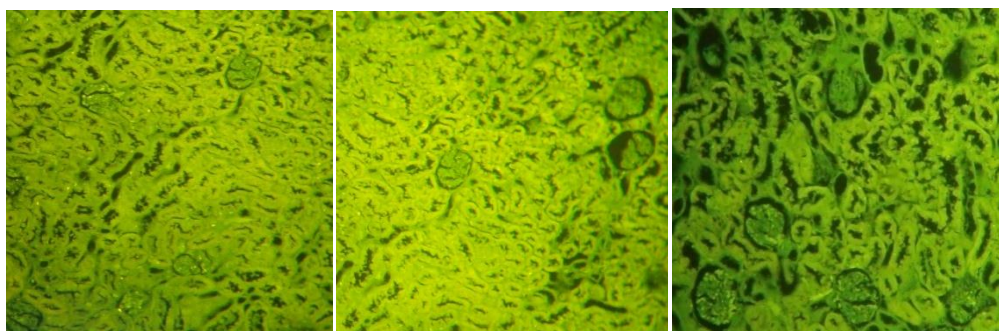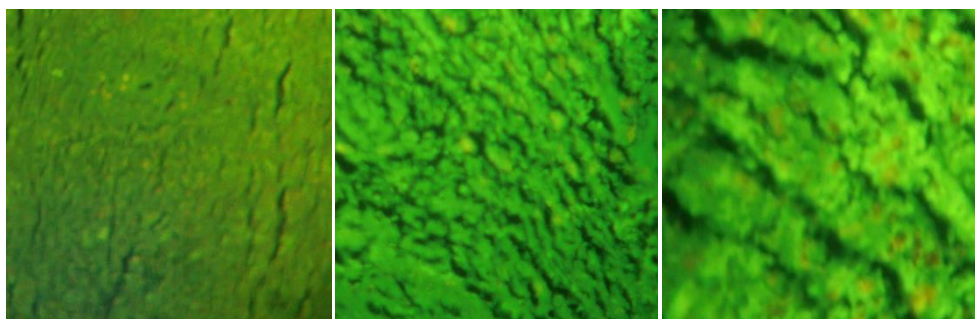
Plain solution DNPs LDNPs

1. Liver
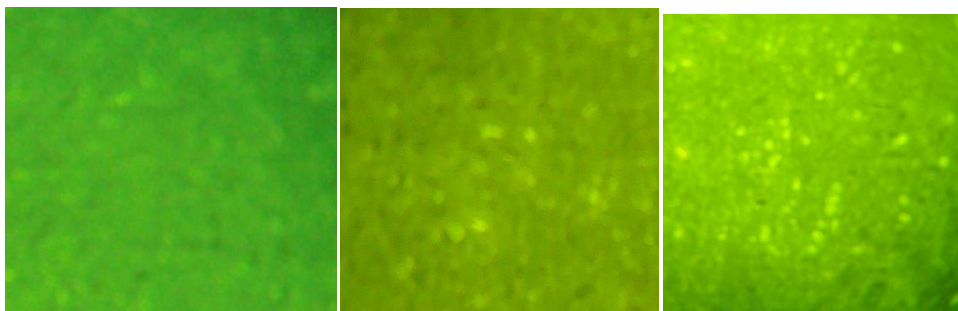
2. Lung

3. Kidney

4. Spleen

Photomicrograph 3: Fluorescent images of different organs of mice after 4 h administration

Ex-vivo cell cytotoxicity

In science, *ex-vivo* refers to experimentation done in or on living tissue in an artificial environment outside the organism. Cell line studies were performed in a view to explore the target ability of the prepared formulation against human cancer cell line HepG2.

Sulforhodamine blue (SRB) colorimetric assay for cytotoxicity screening

The SRB assay is an indirect measure of cell growth, which uses total cellular protein as a surrogate for cell number. The assay counts on the ability of SRB to bind to protein components of cells that have

been fixed to tissue culture plates by trichloroacetic acid (TCA). SRB is a bright pink aminoxanthane dye with two sulfonic acid that bind to basic amino acid residues under mild acidic conditions. The amount of dye extracted from stained cells is directly proportional to cell mass.

Experimental procedure for SRB assay

The cell lines HepG2 were grown in RPMI 1640 medium containing 10% fetal bovine serum and 2 mmol L-glutamine. For present screening experiment, cells were inoculated into 96 well microtiter plates in 100 μl at plating densities as shown in the study details above, depending on the doubling time of individual cell lines. After cell inoculation, the microtiter plates were incubated at 37 °C, 5% CO_2, 95% air and 100% relative humidity for 24 h prior to addition of experimental drugs.

After 24 h, one 96 well plate containing 5×10^3 cells/well was fixed *in situ* with TCA, to represent a measurement of the cell population at the time of drug addiction (Tz). Experimental drugs were initially solubilized in dimethyl sulfoxide at 100 mg/ml and diluted to 1 mg/ml using water and stored frozen prior to use. At the time of drug addition, an aliquote of frozen concentrate (1 mg/ml) was thawed and diluted to 100 μg/ml, 200 μg/ml, 400 μg/ml and 800 μg/ml with complete medium containing test article. Aliquots of 10 μl of these different drug dilutions were added to the appropriate microtiter wells already containing 90 μl of medium, resulting in the required final drug concentrations i.e.10 μg/ml, 20 μg/ml, 40 μg/ml, 80 μg/ml [45].

Endpoint measurement

After compound addition, plates were incubated at standard conditions for 48 h and assay was terminated by the addition of cold TCA. Cells were fixed *in situ* by the gentle addition of 50 μl of cold 30 % (w/v) TCA (final concentration, 10 % TCA) and incubated for 60 min at 4 °C. The supernatant was discarded; the plates were washed five times with tap water and air dried. Sulforhodamine B (SRB)

solution (50 μl) at 0.4 % (w/v) in 1 % acetic acid was added to each of the wells, and plates were incubated for 20 min at room temperature. After staining, unbound dye was recovered and the residual dye was removed by washing five times with 1 % acetic acid. The plates were air dried. Bound stain was subsequently eluted with 10 mmol trizma base, and the absorbance was read on a plate reader at a wavelength of 540 nm with 690 nm reference wavelength.

Percent growth was calculated on a plate-by-plate basis for test wells relative to control wells. Percent Growth was expressed as the ratio of average absorbance of the test well to the average absorbance of the control wells ×100.

Using the six absorbance measurements [time zero (Tz), control growth (C), and test growth in the presence of drug at the four concentration levels (Ti)], the percentage growth was calculated at each of the drug concentration levels. Percentage growth inhibition was calculated as:

[(Ti-Tz)/(C-Tz)] × 100 for concentrations for which Ti>/=Tz (Ti-Tz) positive or zero, [(Ti-Tz)/Tz] × 100 for concentrations for which Ti<Tz. (Ti-Tz) negative

The dose response parameters were calculated for each test article. Growth inhibition of 50% (GI_{50}) was calculated from [(Ti-Tz)/(C-Tz)] x 100 = 50, which is the drug concentration resulting in a 50% reduction in the net protein increase (as measured by SRB staining) in control cells during the drug incubation. The drug concentration resulting in total growth inhibition (TGI) was calculated from Ti = Tz. The LC_{50} (concentration of drug resulting in a 50% reduction in the measured protein at the end of the drug treatment as compared to that at the beginning) indicating a net loss of cells following treatment was calculated from [(Ti-Tz)/Tz] x 100 =-50. Values were calculated for each of these three parameters if the level of activity was reached; however, if the effect was not reached or was exceeded, the values for that parameter were expressed as greater or less than the maximum or minimum concentration tested [46].
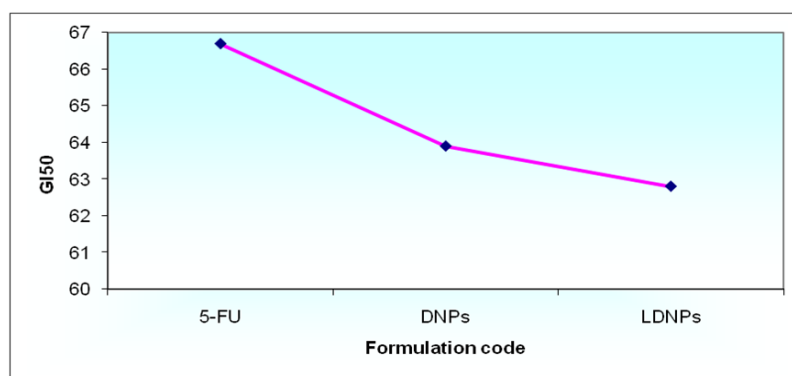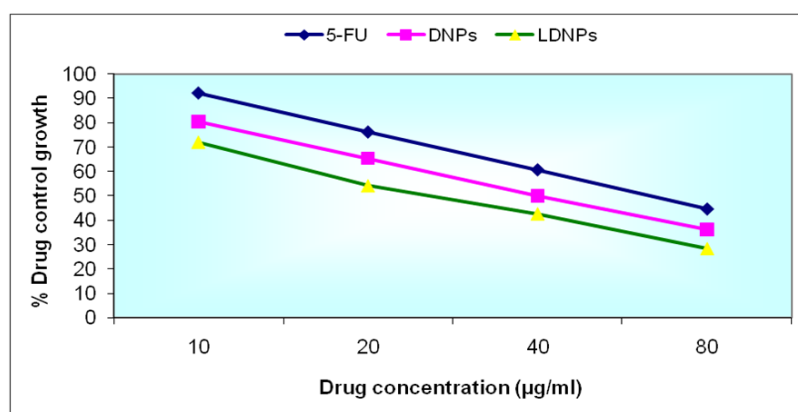

Fig. 8: Growth curve: Human hepatoma cell line HepG2

Fig. 9: Showing percent control growth v/s concentration

RESULTS AND DISCUSSION

Preparation of plain nanoparticles was carried out using the emulsification–diffusion method which involved the diffusion of the organic solvent in to aqueous phase, drug was dissolved in PBS (7.4)/water and subsequently added to aqueous phase containing pluronic F-68. Organic phase containing PLGA/conjugate was injected in to the aqueous phase, following different formulation steps as given in scheme 1.

The final nanoparticle dispersion was filtered through a syringe filter (0.22 μm) various formulation variables i.e. polymer concentration, stabilizer concentration, amount of drug and process variables i.e. stirring speed, stirring time and sonication time were considered to optimize PLGA nanoparticle formulation.

Optimization of the polymer concentration is the first step during the study and it was performed by varying the polymer concentration where as keeping other variables constant. The prepared formulation was optimized on the basis of particle size and polydispersity index. It was observed that the size of particles increased on increasing polymer concentration and it was found to be 106.24±2.1 at 1% polymer concentration where as the polydispersity index was 0.361 at same concentration of polymer. Hence, it was inference that with increase in polymer concentration viscosity of the solution increases, which in turn results bigger size nanoparticles. The polydispersity index is reduced on increasing its concentration from 0.5 to 1.0 while PDI increases on further increase in the polymer concentration. This caused due to increase in viscosity on increasing the polymer to 1.5% that produce hindrance in the movement or diffusion of solvent and produced bigger sized particles. Optimized formulation NP-2 was selected for further optimization of stabilizer concentration. It was observed that the particle size decreased when concentration of stabilizer increases, this may be due to decrease in surface tension and development of charge over the particles in the system because of presence of stabilizer. At 1% stabilizer concentration PDI is 0.321. If the concentration of stabilizer increases beyond 1% the gradual increase in particle size was observed which could be formation of micellar structure of pluoronic F-68 and increases the PDI. Hence, 1% pluoronic F-68 concentration was taken as optimized parameter. So NP2S-2 was taken for further optimization.

Amount of drug was optimized on the basis of particle size and percentage entrapment efficiency. It was observed that on increasing the amount of drug, the entrapment efficiency increased up to 10 mg of drug while on further increasing the amount of drug, the entrapment is not increase. This could be due to saturation of drug with the polymer. Same effect was observed on the particle size also. On the basis of above parameters formulation NP2S2D-2 was selected for further optimization of process variables. Formulation NP2S2D2S2S-2 showed varied effects on varying stirring speed, stirring time and sonication time.

It was observed that as on increasing the stirring speed from 2000 to 3000 rpm, and increasing the stirring time 2 hr to 3 hr the size of nanoparticles was decrease and drug entrapment efficiency was increased. This decrease in size of nanoparticles could be due to high shear force applied to the dispersion. Due to decrease in size the surface area of NPs was increased which in turn increased the drug entrapment efficiency. But beyond 3000 rpm and 3 hr of stirring speed, the size of NPs is reduced which are unstable and form aggregates which results increase in size. Similar effect was observed on varying the sonication time, the decrease in entrapment efficiency was observed due to loss of entrapped drug during reduction of size of NPs.

The conjugation of lactobionic acid with PLGA polymer was proved by FTIR. In EDA conjugated PLGA one peak at 1642.2 cm^{-1}was found which indicates the C=O stretching in amide, peak 3432.0 cm^{-1}represents N-H stretching and peak 1635.3 cm^{-1}N-H bending in amide. In Lactobionic-EDA-PLGA, the peak 1639.6 cm^{-1}and 1635.4 cm^{-1}represent C=O stretching in amide bond of lactobionic ethylene diamine PLGA conjugation, peak 3358.9 cm^{-1}and 3352.3 cm^{-1}represents N-H stretching in amide bond, peak 1375.6 cm^{-1}represents O-H bending in alcohol and peak at 1218.7 cm^{-1}represents C-O stretching in alcohol.

Hence on the basis of above results and observations LDNPs was selected as an optimized formulation for characterization and *in vitro* drug release.

Particle size and zeta potential of the nanoparticle were determined by zetasizer showed that particles are in nano range (blow 200 nm) and have acceptable range of zeta potential.

Shape and surface morphology were determined by TEM and SEM analysis. Transmission electron microscopic image of unconjugated showed that particles are spherical in shape and do not show considerable variation in shape. SEM image of nanoparticles was showing smooth surfaces.

Entrapment efficiency was determined using sephadex G-50 column which was found to be 63.46±1.7 and 60.23±1.3 for DNPs and LDNPs, respectively.

The *in vitro* release profiles of entrapped drug from formulations were determined using dialysis membrane. The percent cumulative drug release from nanoparticles in PBS (pH7.4) at different time intervals was recorded and reflecting sustained release of drug from formulation.

For stability studies, the NP2S2D2S2S-2 is stored at the temperatures 4±1 °C and room temperature. Analyzed the particle size and residual drug content of formulations after the time intervals of 10, 20, 30, 45 and 60 d of storage and optimal storage condition was established.

Upon storage, the particle size was found to increase at high temperature compared to low temperature; it may be due to the aggregation of the particles. Because at high temperature, accelerated collisions of particles increased leads to increasing in the kinetic energy, which forms nanoparticle aggregation.

The percent of residual drug remaining in NP2S2D2S2S-2 after storing at room temperature and low temperature was calculated by assuming the initial drug content as 100%. The residual drug content of formulations stored at room temperature were found to be have more drug loss compared to the formulations stored at 4±1 °C, which indicated that the formulations tend to degrade more at higher temperature.

Hence, the stability studies are indicating that the formulation stored at 4±1 °C was more stable than the formulation stored at room temperatures.

For the *in vivo* performance, the drug blood level studies of the formulations were considered. The formulations were predialyzed to remove unentrapped drug and drug concentration equivalent to that of free drug was given to the mice by intravenous route. The concentration of drugs in the body depends upon its release, biodistribution, metabolism and excretion from the body. In case of free drug maximum dose of drugs was recovered in serum after 15 min. These results clearly indicated a drastic reduction in serum concentration of free drug in NPs formulation and may be accounted for the fact that the most of the drug present in blood was entrapped in the NPs.

In vivo fate of nanoparticles suggests that receptor mediated uptake of nanoparticles by ASGP-R will occur and due to its sustained drug delivery, drug molecule will be available for longer period of time.

In case of LDNPs 37.52±0.68% of 5-FU found in liver, where as 1.03±0.14%, 5.83±0.03%, 3.92±0.01% were found in kidney, lung and spleen, respectively after 24 h of administration (table 7.1 and 7.2, fig 7.1 and 7.2). Besides the distribution of drug to liver was increased from LDNPs as compared to that of 5-FU solution and DNPs. LDNPs reduced the accumulation of drug in kidney as compared to 5-FU solution and DNPs. This may be due to the fact that receptors for galactose are present in liver.

The alteration in the % concentration of 5-FU by different formulation is due to difference in their bio distribution properties. When 5-FU given by i. v. route it distributed by blood circulation in to all organs, it goes in to kidney and retained there in higher amount and become the cause of renal toxicity. But when DNPs were

given, because of these size (around 200 nm), these are taken up by passive targeting and when 5-FU loaded (LDNPs) were given, they are selectively taken up by ASGP-R, exclusively present on liver parenchymal cells, because of galactose, there receptors have taken up LDNPs by receptor mediated endocytosis and retained the drug in the liver. These data clearly indicate that conjugation of galactose containing lactobionic acid with PLGA entrapping 5-FU increases the chances of drug to reach in the liver in large concentration as compared to other organs.

Fluorescence microscopy was performed to establish a qualitative estimation of nanoparticle formulations targeted to various organs. FITC loaded DNPs and LDNPs were administered intravenously to mice through tail vein. The mice were sacrificed after 4 h and organs were excised and microtomy was performed. The photomicrographs were taken through fluorescent microscope. LDNPs shows better uptake in liver because of ASGP-R receptors as compared to DNPs and plain solution.

Performed experiment on human hepatoma cell line HepG2 by SRB assay clearly suggests a dose dependent cytotoxicity response i.e. decrease in cell survival fraction with increasing concentration of drug. It was observed that LDNPs exhibited significantly higher cytotoxicity in comparison to plain 5-FU and DNPs.

The results showed that plain drug solution have least cytotoxicity with GI_{50}, 66.7 µg/ml. This might be due to lesser uptake of drug after 48 h incubation with the cell line. In case of DNPs, LDNPs higher cytotoxic effects were recorded. GI_{50} values of above formulations were found to be 63.9, 62.8 µg/ml respectively.

The DNPs and LDNPs were more cytotoxic as compared to plain 5-FU because of small size of DNPs increase adsorption at the cell surface and asialoglycoprotien receptors are over expressed on cancerous cells which help in direct internalization of conjugated nanoparticles (LDNPs).

The present work demonstrates the suitability of lactobionic conjugated nanoparticles encapsulating 5-FU over other formulations as an optimum delivery system for tumor targeting.

CONCLUSION

Lactobionic acid conjugated nanoparticles prepared showed great potential as a targeted drug delivery system and have tremendous useful properties not seen in any other delivery module. Some properties that make them a suitable carrier are high drug loading, good targetibility and excellent biocompatibility. The proposed targeting strategy enhanced the therapeutic index of conventional anticancer drug as well as reduced its cytotoxic effects to normal cells resulting in potential drug delivery system.

FUNDING

AUTHORS CONTRIBUTIONS

All the authors have contributed equally.

CONFLICT OF INTERESTS

Declared none

REFERENCES

1. Das S, Deshmukh R, Jha AK. Role of natural polymers in the development of multiparticulate systems for colon drug targeting. Syst Rev Pharm. 2010;1(1):79-85. doi: 10.4103/0975-8453.59516.
2. Allemann E, Gurny R, Doelkar E. Drug loaded nanoparticles preparation method and drug targeting tissues. Eur J Pharm Biopharm. 1993;39:173-91.
3. Banfi A, Degenfeld G, Blau HM. Critical role of microenvironmental factors in angiogenesis. Curr Ather Rep. 2005;7:227-34.
4. Calvo J, Akerman ME, Laakkonen P. Nanocrystal target *in vivo*. Proc Natl Acad Sci USA. 2001;99:12613-23.
5. Ciechanover A, Schwartz AL, Lodish HF. Sorting and recycling of cell surface receptors and endocytosed ligands: the asialoglycoprotein and transferrin receptors. J Cell Biochem.

6. 1983;23(1-4):107-30. doi: 10.1002/jcb.240230111, PMID 6327736.
6. Crowther M, Brown NJ, Bishop ET, Lewis CE. Microenvironmental influence on macrophage regulation of angiogenesis in wounds and malignant tumors. J Leukoc Biol. 2001;70(4):478-90. PMID 11590184.
7. Davis BG, Robinson MA. Drug delivery systems based on sugar-macromolecule conjugates. Curr Opin Drug Discov Devel. 2002;5(2):279-88. PMID 11926134.
8. De Abrew SD. Assays for transferrin and transferrin receptors in tumour and other mouse tissues. Int J Nucl Med Biol. 1981;8(4):217-21. doi: 10.1016/0047-0740(81)90025-5, PMID 6276310.
9. Earp HS, Dawson TL, Li X, Yu H. Heterodimerization and functional interaction between EGF receptor family members: A new signaling paradigm with implications for breast cancer research. Breast Cancer Res Treat. 1995;35(1):115-32. doi: 10.1007/BF00694752, PMID 7612898.
10. Engers R, Gabbert HE. Mechanisms of tumor metastasis: cell biological aspects and clinical implications. J Cancer Res Clin Oncol. 2000;126(12):682-92. doi: 10.1007/s004320000148, PMID 11153140.
11. Fallon RJ, Schwartz AL. Asialoglycoprotein receptor phosphorylation and receptor-mediated endocytosis in hepatoma cells. Effect of phorbol esters. J Biol Chem. 1988;263(26):13159-66. doi: 10.1016/S0021-9258(18)37685-3, PMID 3166456.
12. Florey K. Analytical profiles drug substances. Vol. 2. New York: Academic Press; 1973. p. 221-40.
13. Folkman J. Incipient angiogenesis. J Natl Cancer Inst. 2000;92(2):94-5. doi: 10.1093/jnci/92.2.94, PMID 10639502.
14. Baban DF, Seymour LW. Control of tumour vascular permeability. Adv Drug Deliv Rev. 1998;34(1):109-19. doi: 10.1016/s0169-409x(98)00003-9, PMID 10837673.
15. Fry DW, White JC, Goldman ID. Rapid separation of low molecular weight solutes from liposomes without dilution. Anal Biochem. 1978;90(2):809-15. doi: 10.1016/0003-2697(78)90172-0, PMID 727510.
16. Gabius HJ, Andre S, Kaltner H, Siebert HC. The sugar code: functional lectinomics. Biochim Biophys Acta. 2002;1572(2-3):165-77. doi: 10.1016/s0304-4165(02)00306-9, PMID 12223267.
17. Garin-Chesa P, Campbell I, Saigo PE, Lewis JL, Old LJ, Rettig WJ. Trophoblast and ovarian cancer antigen LK26. Sensitivity and specificity in immunopathology and molecular identification as a folate-binding protein. Am J Pathol. 1993;142(2):557-67. PMID 8434649.
18. Gref R, Minamitake Y, Peracchia MT, Trubetskoy V, Torchilin V, Langer R. Biodegradable long-circulating polymeric nanospheres. Science. 1994;263(5153):1600-3. doi: 10.1126/science.8128245, PMID 8128245.
19. Gupta MK, Qin RY. Mechanism and it's regulation of tumor induced angiogenesis. World J Gastroenterol. 2005;9:1144-55.
20. Laroui, Dalmasso, Nguyen, Yutao Yan, Shanthi V Sitaraman, Merlin. Drug-loaded nanoparticles targeted to the colon with polysaccharide hydrogel reduce colitis in a mouse model. Gastroenterology. 2010;138(3):843-53.e1. doi: 10.1053/j.gastro.2009.11.003, PMID 19909746.
21. Han JH, Oh YK, Kim DS, Kim CK. Enhanced hepatocyte uptake and liver targeting of methotrexate using galactosylated albumin as a carrier. Int J Pharm. 1999;188(1):39-47. doi: 10.1016/s0378-5173(99)00206-9, PMID 10528081.
22. Indian Pharmacopoiea. Vol. 1. New Delhi: government of India, ministry of health and family welfare; 1996. p. 323.
23. Kim IS, Kim SH. Development of polymeric nanoparticulate drug delivery systems: evaluation of nanoparticles based on biotinylated poly (ethylene glycol) with sugar moiety. Int J Pharm. 2003;257(1-2):195-203. doi: 10.1016/s0378-5173(03)00128-5, PMID 12711174.
24. Kalsi PS. Spectroscopy of organic compounds. 6th ed. New age international Pvt. Ltd. New Delhi; 2007. p. 66-172.
25. Kannagi R, Izawa M, Koike T, Miyazaki K, Kimura N. Carbohydrate-mediated cell adhesion in cancer metastasis and angiogenesis. Cancer Sci. 2004;95(5):377-84. doi: 10.1111/j.1349-7006.2004.tb03219.x, PMID 15132763.

26. Yang J, Han S, Zheng H, Dong H, Liu J. Preparation and application of micro/nanoparticles based on natural polysaccharides. Carbohydr Polym. 2015;123:53-66. doi: 10.1016/j.carbpol.2015.01.029, PMID 25843834.

27. Kilpatrick DC. Mannan-binding lectin: clinical significance and applications. Biochim Biophys Acta. 2002;1572(2-3):401-13. doi: 10.1016/s0304-4165(02)00321-5, PMID 12223282.

28. Kim IS, Jeong YI, Cho CS, Kim SH. Core-shell type polymeric Nano particles composed of poly (L-lactic acid) and poly (N-isopropylacrylamide). Int J Pharm. 2002;211:1-8.

29. Larsen AK, Escargueil AE, Skladanowski A. Resistance mechanisms associated with altered intracellular distribution of anticancer agents. Pharmacol Ther. 2000;85(3):217-29. doi: 10.1016/s0163-7258(99)00073-x, PMID 10739876.

30. Lee JH, Ku JL, Park YJ, Lee KU, Kim WH, Park JG. Establishment and characterization of four human hepatocellular carcinoma cell lines containing hepatitis B virus DNA. World J Gastroenterol. 1999;45(4):289-95. doi: 10.3748/wjg.v5.i4.289, PMID 11819450.

31. Rani M, Agarwal A, Negi YS. Chitosan based hydrogel polymeric beads–as drug delivery system. Bio-Resour. 2010;5(4).

32. Nicolson G. Molecular cell biology and cancer metastasis. An interview with Garth Nicolson. Int J Dev Biol. 2004;48(5-6):355-63. doi: 10.1387/ijdb.041803mm, PMID 15349811.

33. Lin X, Wu Q, Chen Z, Gong X, Lin X. Preparation, characterization and controlled release of liver-targeting nanoparticles from the amphiphilic random copolymer. Polymer. 2008;49(22):4769-75. doi: 10.1016/ j.polymer.2008.09.006.

34. Molema G, de Leij LFMH, Meijer DKF. Tumor vascular endothelium: barrier or target in tumor directed drug delivery and immunotherapy. Pharma Res. 1997;14(1):2-10. doi: 10.1023/a:1012038930172, PMID 9034214.

35. Nakashima Matsushita N, Homma T, Yu S, Matsuda T, Sunahara N, Nakamura T, Tsukano M, Ratnam M, Matsuyama T. Selective expression of folate receptor β and its possible role in methotrexate transport in synovial macrophages from patients with rheumatoid arthritis. Arthritis Rheum. 1999;42(8):1609-16. doi: 10.1002/1529-0131(199908)42:8<1609::AID-ANR7>3.0.CO;2-L, PMID 10446858.

36. Pan H, Gao F, Papageorgis P, Abdolmaleky HM, Faller DV, Thiagalingam S. Aberrant activation of gamma-catenin promotes genomic instability and oncogenic effects during tumor progression. Cancer Biol Ther. 2007;6(10):1638-43. doi: 10.4161/cbt.6.10.4904, PMID 18245958.

37. Ramaa CS, Tilekar KN, Patil VM. Liver cancer: different approaches for targeting. Int J Pharm Technol. 2010:834-42.

38. Nakayama M, Abiru N, Moriyama H, Babaya N, Liu E, Miao D, Yu L, Wegmann DR, Hutton JC, Elliott JF, Eisenbarth GS. Prime role for an insulin epitope in the development of type 1 diabetes in NOD mice. Nature. 2005;435(7039):220-3. doi: 10.1038/nature03523, PMID 15889095.

39. Saif MW. Pancreatic cancer: highlights from the 42nd annual meeting of the American Society of Clinical Oncology, 2006. JOP. 2006;7(4):337-48. PMID 16832131.

40. Sarkar Biresh K, Devananda J, Angshu B. New drug delivery system. IJRAP. 2011;2(5):1513-7.

41. Schwartz AL, Rup D, Lodish HF. Difficulties in the quantification of asialoglycoprotein receptors on the rat hepatocyte. J Biol Chem. 1980;255(19):9033-6. doi: 10.1016/S0021-9258(19)70522-5, PMID 7410410.

42. Huang W, Wang W, Wang P, Tian Q, Zhang C, Wang C. Glycyrrhetinic acid-modified poly(ethylene glycol)–b-poly(γ-benzyl l-glutamate) micelles for liver targeting therapy. Acta Biomaterialia. 2010;6(10):3927-35. doi: 10.1016/ j.actbio.2010.04.021.

43. Toffoli G, Cernigoi C, Russo A, Gallo A, Bagnoli M, Boiocchi M. Overexpression of folate binding protein in ovarian cancers. Int J Cancer. 1997;74(2):193-8. doi: 10.1002/(sici)1097-0215(19970422)74:2<193::aid-ijc10>3.0.co;2-f, PMID 9133455.

44. Vyas SP, Khar RK. Targeted and controlled drug delivery novel carrier systems. CBS publishers and distributors. New Delhi. 2001;331-84.

45. Weigel PH, Yik JHN. Glycans as endocytosis signals: the cases of the asialoglycoprotein and hyaluronan/chondroitin sulfate receptors. Biochim Biophys Acta. 2002;1572(2-3):341-63. doi: 10.1016/s0304-4165(02)00318-5, PMID 12223279.

46. Vichai V, Kirtikara K. Sulforhodamine B colorimetric assay for cytotoxicity screening Nature. Nat Protoc. 2006;1(3):1112-6. doi: 10.1038/nprot.2006.179, PMID 17406391.